Synthesis, Structural Characterization and Thermal Reactivities of Osmium Carbonyl Clusters containing 4,6-Dimethylpyrimidine-2-thione†

Yat-Kun Au, Kung-Kai Cheung and Wing-Tak Wong*
Department of Chemistry, The University of Hong Kong, Pokfulam Road, Hong Kong

The reaction of the labilized cluster $[Os_3(CO)_{10}(MeCN)_2]$ and bis(4,6-dimethylpyrimidin-2-yl) disulfide affords two major products $[Os_3(CO)_{10}(\mu\text{-dmpymt})_2]$ **1** (36%) and $[Os_3(CO)_{10}(\mu\text{-SH})(\mu\text{-dmpymt})]$ **2** (19%) (dmpymt = 4,6-dimethylpyrimidine-2-thione). Cluster **2** is formed from C–S bond cleavage of one of the dmpymt ligands at ambient conditions. Thermolysis of cluster **1** in *n*-heptane (98 °C) for 1 h produces an isomeric cluster of **1**, $[Os_3(CO)_{10}(\mu\text{-dmpymt})_2]$ **3** (62%), which contains two dmpymt ligands co-ordinated across the same non-bonding Os···Os edge. Thermolysis of cluster **3** in *n*-heptane for 2 h affords the cluster $[Os_3(CO)_9(\mu\text{-dmpymt})(\mu_3\text{-}\eta^2\text{-dmpymt})]$ **4** as the major product (42%) in addition to a minor product $[Os_3(CO)_8(\mu\text{-}\eta^2\text{-dmpymt})(\mu_3\text{-}\eta^2\text{-dmpymt})]$ **5** (9%). Cluster **4** contains two dmpymt moieties co-ordinating in μ and $\mu_3\text{-}\eta^2$ modes respectively. Cluster **5** has two dmpymt moieties bonding in the $\mu_3\text{-}\eta^2$ and $\mu\text{-}\eta^2$ modes respectively. Further thermolysis of cluster **4** in *n*-octane (125 °C) leads to a much higher yield of cluster **5** (60%) at the expense of cluster **4**. Chemical activation of cluster **1** using Me_3NO in CH_2Cl_2 at −78 °C also produces clusters **4** and **5** in 20 and 15% yield respectively. A new, orange product (31%) is also formed but remains uncharacterized. When cluster **4** is allowed to stand under ambient conditions over a period of ten days, it isomerizes to the cluster $[Os_3(CO)_9(\mu\text{-dmpymt})(\mu\text{-}\eta^2\text{-dmpymt})]$ **6** in almost quantitative yield (87%). Cluster **6** contains one dmpymt ligand co-ordinating in the $\mu\text{-}\eta^2$ five-electron donating mode. Cluster **5** undergoes carbonylation to form cluster **4** (62%) under a CO atmosphere in CH_2Cl_2 while cluster **4** also changes back to cluster **3** (47%) in refluxing *n*-hexane (69 °C) under a CO atmosphere. Formation of clusters **3**–**5** is thus reversible. Mechanisms for the formation of **3**, **4** and **6** have also been proposed. All the clusters **1**–**6** isolated have been fully characterized by conventional spectroscopic methods as well as single-crystal X-ray analyses.

The chemistry of transition-metal clusters with heterocyclic organic molecules has received much attention over the past decade.[1–5] The presence of such heteroatoms as oxygen,[6] sulfur,[6–8] nitrogen[9–11] and phosphorus[12] has introduced novel reactivities and frequently stabilizes the metal cluster framework with respect to degradational fragmentation when subjected to forcing reaction conditions. Reactivities of organic heterocyclic molecules containing N and S atoms such as pyridine-2-thione,[13] thioamide[14] as well as pyrimidine-2-thione[15] towards metal carbonyl clusters are therefore of considerable interest. We have reported recently the co-ordination ability and the chemical properties of 4,6-dimethylpyrimidine-2-thione (dmpymt) towards osmium and ruthenium carbonyl clusters. The cluster-assisted C–S bond cleavage at ambient conditions has also been demonstrated.[15]

In this paper, we describe the reactions of bis(4,6-dimethylpyrimidin-2-yl) disulfide (Fig. 1), the oxidation product of dmpymt, with osmium carbonyl clusters. Related works on organic molecules of the type R–X–X–R′ (R, R′ = alkyl or aryl) with X = S or Se have been reported by Deeming and Vaish[16] and by Lewis and co-workers,[17,18] respectively.

Similar to pyridine-2-thione and thioamide molecules, pyrimidine-2-thione exists in tautomeric equilibrium (–N=C–SH ⇌ –NH–C=S) in solution with the thione form dominating in the solid state.[19] Pyrimidine-2-thione is known to be able to act as a monodentate ligand through the sulfur atom **A**,[20] as a chelating ligand through the sulfur and nitrogen atoms **B**,[21] as a bridging ligand through the sulfur atom **C**[15] and as a bridging ligand through its nitrogen and sulfur atoms **D** and **E**,[15,22] see Fig. 2.

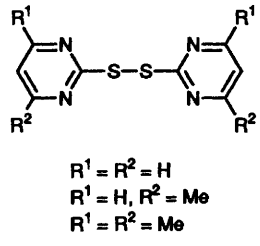

$R^1 = R^2 = H$
$R^1 = H, R^2 = Me$
$R^1 = R^2 = Me$

Fig. 1 Bipyrimidin-2-yl disulfide type ligands

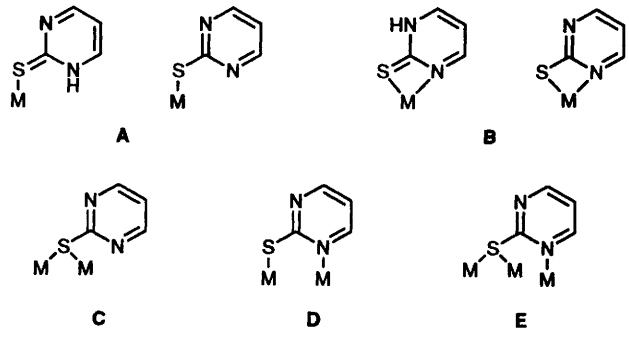

Fig. 2 Some co-ordination modes of Hpymt ligands

† *Supplementary data available:* see Instructions for Authors, *J. Chem. Soc., Dalton Trans.*, 1995, Issue 1, pp. xxv–xxx.

Experimental

General Conditions.—All operations were carried out under a dinitrogen atmosphere using standard Schlenk techniques, unless stated otherwise. Solvents were purified and distilled from the appropriate drying agents and stored under nitrogen prior to use. Products were separated by thin layer chromatography (TLC) on silica gel (type 60) GF_{254} Merck 7730 in air.

Instrumentation.—Infrared spectra were recorded on a BIO-RAD FTS-7 or SHIMADZU 470 IR spectrophotometer in CH_2Cl_2 or *n*-hexane. ^1H NMR spectra were recorded in CD_2Cl_2 or $CDCl_3$ on a JEOL GSX 270 FT-NMR spectrometer. Mass spectra were recorded on a Finnigan MAT 95 spectrometer with fast atom bombardment techniques using *m*-nitrobenzyl alcohol as matrix.

Reagents.—The compound $[Os_3(CO)_{10}(MeCN)_2]$ was prepared according to a published procedure.[23] Bis(4,6-dimethylpyrimidin-2-yl) disulfide was prepared by treating 4,6-dimethylpyrimidine-2-thione·HCl with sodium nitrite in water and was recrystallized from ethanol–light petroleum (b.p. 40–60 °C) (1:1);[24] $[Os_3(CO)_{12}]$ (Strem) was used as received. Trimethylamine *N*-oxide (Me_3NO) was sublimed immediately prior to use.

Reaction of $[Os_3(CO)_{10}(MeCN)_2]$ *with Bis(4,6-dimethylpyrimidin-2-yl) Disulfide.*—A solution of $[Os_3(CO)_{10}(MeCN)_2]$ (100 mg, 0.107 mmol) in CH_2Cl_2 (25 cm^3) was stirred with an excess of bis(4,6-dimethylpyrimidin-2-yl) disulfide (30.62 mg, 0.110 mmol) at room temperature. The initial yellow solution gradually changed to orange upon stirring. The stirring was continued for 1 h and the solvent was then removed under reduced pressure. The residue was redissolved in CH_2Cl_2 (2 cm^3) and separated by preparative TLC using eluent (acetone–*n*-hexane, 2:8 v/v) to give four bands. The first yellow band ($R_f \approx 0.7$) was extracted with acetone and gave $[Os_3(CO)_{10}(\mu\text{-SH})(\mu\text{-dmpymt})]$ **2** in 19% yield. Cluster **2** was recrystallized from CH_2Cl_2–*n*-hexane mixtures at −10 °C to give pale yellow needles. The second yellow band ($R_f \approx 0.5$) gave $[Os_3(CO)_{10}(\mu\text{-dmpymt})_2]$ **1** in 36% yield and was crystallized from CH_2Cl_2–*n*-hexane at − 20 °C to give yellow crystals. Attempts to purify the remaining two bands by repeated TLC was unsuccessful and they remained uncharacterized.

Thermolysis of $[Os_3(CO)_{10}(\mu\text{-dmpymt})_2]$ **1**.—A suspension of cluster **1** (0.10 g, 0.09 mmol) in distilled *n*-heptane (98 °C) was refluxed for 1 h under nitrogen. The solution gradually changed from light to dark yellow. Thermolysis was continued until no starting materials remained (IR monitoring). The solvent was then removed *in vacuo*. The dark yellow residue was redissolved in CH_2Cl_2 (2 cm^3) and TLC separation (CH_2Cl_2–*n*-hexane, 5:5 v/v) afforded one major pale yellow band. Crystallization from CH_2Cl_2–pentane gave very pale yellow microcrystals of the isomeric cluster **3** (62%).

Thermolysis of $[Os_3(CO)_{10}(\mu\text{-dmpymt})_2]$ **3**.—A very pale yellow solution of cluster **3** (0.05 g, 0.044 mmol) in distilled *n*-heptane was refluxed for 2 h under nitrogen. The solvent was then removed *in vacuo*. The residue was washed with diethyl ether (3 × 5 cm^3) and then redissolved in CH_2Cl_2 (2 cm^3). Separation by TLC (CH_2Cl_2–*n*-hexane, 4:6 v/v) afforded the pale orange cluster $[Os_3(CO)_9(\mu\text{-dmpymt})(\mu_3\text{-}\eta^2\text{-dmpymt})]$ **4** (42%) as the major product. Crystals of **4** were obtained from a *n*-hexane solution at −20 °C. A minor product $[Os_3(CO)_8(\mu\text{-}\eta^2\text{-dmpymt})(\mu_3\text{-}\eta^2\text{-dmpymt})]$ **5** (9%) was crystallized from CH_2Cl_2–*n*-hexane at −20 °C to give deep orange crystals of **5**.

Thermolysis of $[Os_3(CO)_9(\mu\text{-dmpymt})(\mu_3\text{-}\eta^2\text{-dmpymt})]$ **4** *in* n-*Octane.*—Cluster **4** (0.05 g, 0.045 mmol) was dissolved in *n*-octane (20 cm^3) and heated under reflux for 30 min under nitrogen during which time the solution changed from yellow to pale orange. IR monitoring indicated the complete disappearance of **4**. The solvent was removed *in vacuo* and the residue was redissolved in 2 cm^3 of CH_2Cl_2. Purification by TLC using CH_2Cl_2–*n*-hexane (5:5 v/v) as eluent gave cluster **5** in 60% yield.

Reaction of Me_3NO *with* $[Os_3(CO)_{10}(\mu\text{-dmpymt})_2]$ **1**.—A suspension of cluster **1** (0.10 g, 0.09 mmol) in CH_2Cl_2 (30 cm^3) was cooled to −78 °C. A CH_2Cl_2 (5 cm^3) solution of Me_3NO (11.25 mg, 0.15 mmol) was added dropwise over 15 min. The mixture was allowed to warm to room temperature and stirred for a further 1 h. The solvent was evaporated *in vacuo* and the products were separated by TLC using CH_2Cl_2–*n*-hexane (2:8 v/v) as eluent, resulting in the isolation of **3** (20%), **4** (15%) and an uncharacterized orange product (31%).

Carbonylation of $[Os_3(CO)_8(\mu\text{-}\eta^2\text{-dmpymt})(\mu_3\text{-}\eta^2\text{-dmpymt})]$ **5**.—Carbon monoxide gas at 1 atm was bubbled through a yellow solution of **5** (0.10 g, 0.09 mmol) in CH_2Cl_2 for 3 h. The solvent was then removed and the residue was redissolved in CH_2Cl_2 (2 cm^3). IR spectroscopy showed the complete conversion of **5** into **4**. TLC separation (CH_2Cl_2–*n*-hexane, 2:8 v/v) afforded the yellow cluster **4** as the only separable product (62%).

Carbonylation of $[Os_3(CO)_9(\mu\text{-dmpymt})(\mu_3\text{-}\eta^2\text{-dmpymt})]$ **4**.—Carbon monoxide gas at 1 atm was bubbled through a yellow solution of **4** (0.05 g, 0.045 mmol) in *n*-hexane under reflux for 3 h. The solvent was then removed *in vacuo* and the residue was redissolved in CH_2Cl_2 (2 cm^3). TLC separation (CH_2Cl_2–*n*-hexane, 2:8 v/v) afforded the yellow cluster **3** as the major separable product (27%).

Isomerization of $[Os_3(CO)_9(\mu\text{-dmpymt})(\mu_3\text{-}\eta^2\text{-dmpymt})]$ **4**.—A solution of cluster **4** (0.05 g, 0.045 mmol) was dissolved in CH_2Cl_2 (5 cm^3)–*n*-heptane (5 cm^3). The conversion was monitored by IR and was completed over a period of 10 days. TLC separation (CH_2Cl_2–*n*-hexane, 2:8 v/v) afforded one major yellow band which was crystallized from CH_2Cl_2 as pale orange crystals of $[Os_3(CO)_9(\mu\text{-dmpymt})(\mu\text{-}\eta^2\text{-dmpymt})]$ **6** (87%).

Crystal Structure Analyses of Clusters **1**–**6**.—Single crystals representative of bulk samples for clusters **1**–**6** suitable for X-ray analysis were obtained by slow evaporation from either *n*-hexane or *n*-hexane–CH_2Cl_2 at −20 °C. Crystals were mounted in air on a glass fibre with epoxy resin. X-Ray diffraction data of clusters **1**, **4** and **5** were collected on an Enraf-Nonius CAD4 diffractometer and of **2**, **3** and **6** on a Rigaku AFC7R diffractometer, all using graphite-monochromated Mo-Kα (λ = 0.710 73 Å) radiation using the ω–2θ scan method. Crystal data of all six clusters are summarized in Table 14. All intensity data were corrected for Lorentz and polarization effects and empirical absorption based on ψ-scans of four to six strong reflections.[25] No decay was observed for any of the crystals. In all six data sets, reflections with $I \geqslant 3\sigma(I)$ were considered observed and used in the structural analyses. The space groups of all six clusters were determined from systematic absences and the structures were solved by direct methods/Patterson and Fourier methods and subsequent refinement by full-matrix least squares on *F* using Enraf-Nonius SDP-1985 programs[26] on a MicroVAX II computer and the TEXSAN software package[27] on a SGI computer respectively. Atomic coordinates of non-hydrogen atoms are listed in Tables 2, 4, 6, 8, 10 and 12. Additional material available from the Cambridge Crystallographic Data Centre comprises H-atom coordinates, thermal parameters and remaining bond lengths and angles.

Table 1 Spectroscopic data for the clusters **1–6**

Cluster	IR, ν(CO)/cm^{-1}	^{1}H NMR	FAB MS (m/z) M^+ [a]
1	2115m, 2068s, 2057m, 2043m, 2034vs, 2016m, 1995m, 1983s, 1962m [b]	6.73 (s, 1 H, aryl H), 6.26 (s, 1 H, aryl H), 2.44 (s, 6 H, CH_3), 2.39 (s, 6 H, CH_3) [c]	1134 (1134)
2	2108w, 2069s, 2060m, 2022vs, 2017m, 2005m, 1988w, 1984w [b]	6.79 (s, 1 H, aryl H), 2.42 (s, 6 H, CH_3), 2.25 (br, 1 H, SH) [c]	1029 (1029)
3	2103m, 2069vs, 2057s, 2012vs, 1978m [d]	6.52 (s, 2 H, aryl H), 2.26 (s, 12 H, CH_3) [e]	1134 (1134)
4	2078m, 2055vs, 2023vs, 1981s, 1954m, 1936m, 1954m, 1936m [d]	6.90 (s, 1 H, aryl H), 6.86 (s, 1 H, aryl H), 2.91 (s, 3 H, CH_3), 2.51 (s, 6 H, CH_3), 2.26 (s, 3 H, CH_3) [e]	1106 (1106)
5	2069m, 2033vs, 1994m, 1980vs, 1964w, 1940m, 1918m [b]	7.22 (s, 1 H, aryl H), 6.89 (s, 1 H, aryl H), 2.90 (s, 3 H, CH_3), 2.54 (s, 6 H, CH_3), 2.29 (s, 3 H, CH_3) [c]	1078 (1078)
6	2096s, 2059s, 2006vs, 1989s, 1922m [d]	6.63 (s, 1 H, aryl H), 6.58 (s, 1 H, aryl H), 2.35 (s, 3 H, CH_3), 2.32 (s, 6 H, CH_3), 2.29 (s, 3 H, CH_3)	1106 (1106)

br = Broad, s = strong, m = medium, w = weak, s = singlet (NMR). [a] Calculated values in parentheses, M^+ = molecular ion (^{192}Os). [b] Recorded in *n*-hexane. [c] Recorded in $CDCl_3$ at 298 K. [d] Recorded in CH_2Cl_2. [e] Recorded in CD_2Cl_2 at 298 K.

Table 2 Atomic coordinates with estimated standard deviations (e.s.d.s) of cluster **1**

Atom	x	y	z	Atom	x	y	z
Os(1)	0.687 72(4)	0.373 79(2)	1.286 50(2)	O(24)	0.174 2(8)	0.456 2(4)	1.229 0(5)
Os(2)	0.295 93(4)	0.347 08(2)	1.350 50(2)	O(31)	0.615(1)	0.258 0(5)	1.052 7(5)
Os(3)	0.453 68(4)	0.309 76(2)	1.201 35(2)	O(32)	0.466(1)	0.169 6(4)	1.274 8(6)
S(1)	0.518 0(3)	0.406 0(2)	1.390 4(2)	O(33)	0.177 4(9)	0.297 1(5)	1.095 8(6)
S(2)	0.515 7(3)	0.426 3(1)	1.191 1(2)	N(1)	0.357 2(9)	0.513 6(5)	1.404 0(5)
C(11)	0.805(1)	0.347 8(6)	1.197 9(7)	N(2)	0.594(1)	0.531 6(5)	1.358 0(5)
C(12)	0.818(1)	0.443 2(7)	1.323 0(8)	N(3)	0.575 4(9)	0.413 8(5)	1.028 2(5)
C(13)	0.754(1)	0.301 4(7)	1.358 8(7)	N(4)	0.694(1)	0.499 1(5)	1.110 2(5)
C(21)	0.387(1)	0.272 6(6)	1.414 8(7)	C(1)	0.485(1)	0.493 1(6)	1.382 3(6)
C(22)	0.199(1)	0.383 9(7)	1.445 7(7)	C(2)	0.332(1)	0.582 1(6)	1.399 3(7)
C(23)	0.148(1)	0.289 7(6)	1.310 5(7)	C(3)	0.438(1)	0.622 6(7)	1.371 4(7)
C(24)	0.223(1)	0.417 6(6)	1.271 9(7)	C(4)	0.567(1)	0.598 1(6)	1.350 6(6)
C(31)	0.557(1)	0.280 6(5)	1.109 4(7)	C(5)	0.191(1)	0.603 1(7)	1.421 5(9)
C(32)	0.461(1)	0.222 2(6)	1.247 9(7)	C(6)	0.681(1)	0.640 6(7)	1.316 1(9)
C(33)	0.278(1)	0.303 0(6)	1.136 8(7)	C(7)	0.605(1)	0.447 2(5)	1.097 0(6)
O(11)	0.877(1)	0.334 5(6)	1.143 4(5)	C(8)	0.648(1)	0.434 4(6)	0.961 3(6)
O(12)	0.907(1)	0.482 4(5)	1.340 4(7)	C(9)	0.745(1)	0.486 0(6)	0.964 9(7)
O(13)	0.792(1)	0.259 6(5)	1.400 4(6)	C(10)	0.763(1)	0.518 5(6)	1.043 0(7)
O(21)	0.439(1)	0.231 8(5)	1.454 5(5)	C(14)	0.615(2)	0.395 2(7)	0.880 8(8)
O(22)	0.134(1)	0.405 8(5)	1.497 1(5)	C(15)	0.864(2)	0.577 0(8)	1.052 2(9)
O(23)	0.058 2(9)	0.253 5(4)	1.284 1(5)				

Results and Discussions

Treatment of $[Os_3(CO)_{10}(MeCN)_2]$ with a stoichiometric amount of bis(4,6-dimethylpyrimidin-2-yl) disulfide at room temperature in CH_2Cl_2 afforded two major products: $[Os_3(CO)_{10}(\mu\text{-dmpymt})_2]$ **1** (36%) and $[Os_3(CO)_{10}(\mu\text{-SH})(\mu\text{-dmpymt})]$ **2** (19%). ^{1}H NMR, IR and FAB mass spectroscopies of **1** all reveal that two dimethylpyrimidine-2-thione (dmpymt) moieties have been co-ordinated to the cluster framework (Table 1). These two dmpymt ligands are most probably derived from S–S bond dissociation of the disulfide ligand. In accordance with previously reported work,[28] the dmpymt ligands are expected to bridge along the same Os–Os edge. However, IR spectroscopy shows that a new molecular structure has been formed based on the ν(CO) absorption band pattern. To establish its molecular structure, a single-crystal X-ray analysis was performed. An ORTEP drawing of **1** is shown in Fig. 3. Final atomic positional parameters are listed in Table 2 and selected bond lengths and angles are listed in Table 3. Cluster **1** consists of an open osmium triangle with the two dmpymt moieties bridging across one bonding and one non-bonding Os–Os edge respectively, both in the bonding mode **C**. Both dmpymt moieties act as a three-electron donor which results in a total of 50 cluster valence electrons and the observation of only two formal Os–Os bonds present in the trinuclear framework is consistent with the electron count. Of the two bridged Os–Os, Os(1)–Os(2) and Os(1)–Os(3), the former

shows a non-bonding distance of 3.891(1) Å whilst the latter bears a typical bonding Os–Os distance of 2.8219(6) Å. This is consistent with the larger Os(1)–S(1)–Os(2) angle [106.0(1)°] as compared with the Os(1)–S(2)–Os(3) angle [72.15(7)°]. The bridged Os(1)–Os(3) edge in turn is shorter than the unsupported Os(2)–Os(3) edge [2.9384(6) Å]. Moreover, the Os(1)–Os(3) distance is slightly shorter than the Os(1)–Os(1*) edge [2.879(1) Å] in $[Os_3(CO)_{10}(\mu\text{-H})(\mu\text{-dmpymt})]$[15] which is also bridged by a hydride ligand in addition to the dmpymt ligand. This is reasonable since bridging hydride has a lengthening effect on metal–metal bonds in metal carbonyl clusters.[29] The dmpymt moiety bridging the Os(1)–Os(3) edge is almost symmetrical [Os(3)–S(2) 2.397(3) Å *vs.* Os(1)–S(2) 2.395(2) Å] as in the case of $[Os_3(CO)_{10}(\mu\text{-H})(\mu\text{-dmpymt})]$.[15] In contrast, the Os(2)–S(1) length [2.445(3) Å] and the Os(1)–S(1) length [2.428(3) Å] spanned by another dmpymt moiety is less symmetrical. Noticeably, the bonding

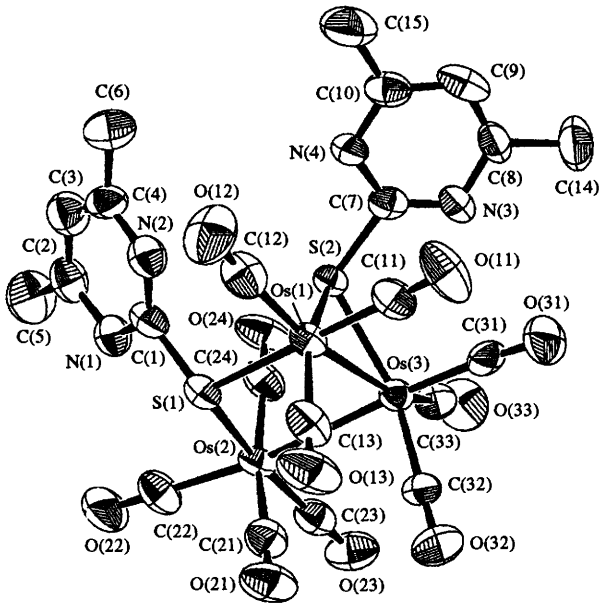

Fig. 3 An ORTEP drawing of $[Os_3(CO)_{10}(\mu\text{-dmpymt})_2]$ **1**

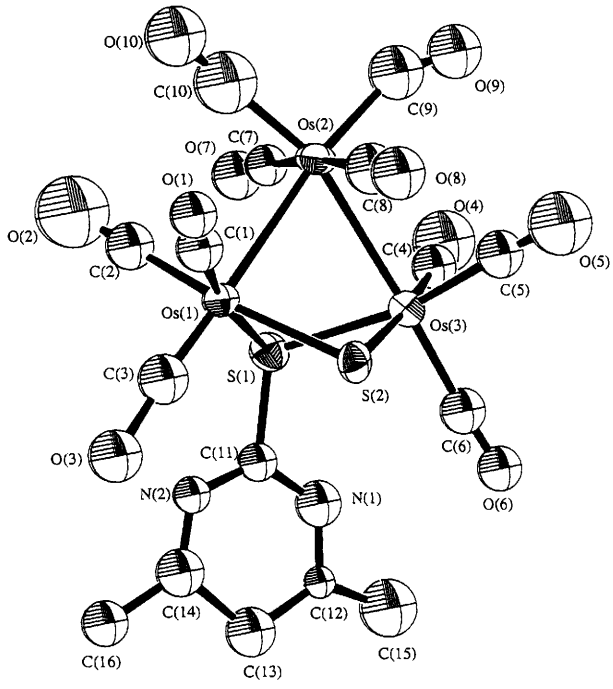

Fig. 4 An ORTEP drawing of $[Os_3(CO)_{10}(\mu\text{-SH})(\mu\text{-dmpymt})]$ **2**

Table 3 Selected bond lengths (Å) and angles (°) of cluster **1**

Os(1)–Os(3)	2.8219(6)	Os(2)–Os(3)	2.9384(6)
Os(1)–S(1)	2.428(3)	Os(1)–S(2)	2.395(2)
Os(2)–S(1)	2.445(3)	Os(3)–S(2)	2.397(3)
S(1)–C(1)	1.76(1)	S(2)–C(7)	1.79(2)
N(1)–C(1)	1.33(1)	N(1)–C(2)	1.38(2)
N(3)–C(7)	1.29(1)	N(3)–C(8)	1.35(1)
N(4)–C(7)	1.33(1)	N(4)–C(10)	1.33(1)
N(2)–C(1)	1.34(1)	N(2)–C(4)	1.35(1)
Os(1)–Os(3)–Os(2)	84.97(2)	Os(3)–Os(1)–S(2)	53.97(6)
Os(1)–S(1)–Os(2)	106.0(1)	Os(2)–Os(3)–S(2)	86.73(7)
Os(1)–S(2)–Os(3)	72.15(7)	Os(3)–Os(1)–S(1)	85.56(6)
Os(3)–Os(2)–S(1)	82.74(6)		

Table 5 Selected bond lengths (Å) and angles (°) of cluster **2**

Os(1)–Os(2)	2.869(2)	Os(2)–Os(3)	2.870(2)
Os(1)–S(2)	2.49(1)	Os(1)–S(1)	2.40(1)
Os(3)–S(2)	2.51(1)	Os(3)–S(1)	2.43(1)
S(1)–C(11)	1.78(4)	N(1)–C(11)	1.28(5)
N(2)–C(11)	1.33(6)		
Os(1)–Os(2)–Os(3)	70.68(6)	Os(1)–S(1)–Os(3)	86.7(3)
Os(1)–S(2)–Os(3)	83.3(3)	Os(2)–Os(1)–S(1)	80.4(3)
Os(2)–Os(3)–S(2)	86.8(3)	Os(2)–Os(1)–S(2)	87.2(3)
Os(2)–Os(3)–S(1)	80.0(3)		

Table 4 Atomic coordinates with e.s.d.s of cluster **2**

Atom	*x*	*y*	*z*	Atom	*x*	*y*	*z*
Os(1)	0.131 5(2)	0.125 02(7)	0.937 9(2)	C(1)	0.138(5)	0.081(2)	0.803(6)
Os(2)	0.129 6(2)	0.202 10(7)	1.167 5(2)	C(2)	0.254(5)	0.170(2)	0.855(6)
Os(3)	0.136 0(2)	0.095 56(7)	1.286 1(2)	C(3)	−0.016(5)	0.161(2)	0.845(5)
S(1)	0.294(1)	0.085 5(4)	1.093(1)	C(4)	0.16(1)	0.261(5)	1.04(1)
S(2)	−0.017 6(10)	0.069 3(5)	1.088(1)	C(5)	−0.065(6)	0.191(2)	1.166(6)
O(1)	0.134(4)	0.040(1)	0.686(4)	C(6)	0.318(4)	0.204(2)	1.170(5)
O(2)	0.324(6)	0.199(2)	0.799(6)	C(7)	0.126(6)	0.248(3)	1.352(7)
O(3)	−0.101(3)	0.183(1)	0.799(3)	C(8)	−0.004(5)	0.119(2)	1.408(6)
O(4)	0.120(5)	0.298(2)	0.949(5)	C(9)	0.258(5)	0.118(2)	1.416(5)
O(5)	−0.177(4)	0.184(2)	1.158(4)	C(10)	0.148(5)	0.024(2)	1.360(5)
O(6)	0.430(3)	0.200(1)	1.171(4)	C(11)	0.328(4)	0.017(2)	1.048(5)
O(7)	0.117(4)	0.252(2)	1.465(5)	C(12)	0.361(3)	−0.067(1)	1.132(4)
O(8)	−0.092(5)	0.131(2)	1.488(5)	C(13)	0.374(5)	−0.088(2)	0.993(6)
O(9)	0.343(5)	0.133(2)	1.488(5)	C(14)	0.351(5)	−0.042(2)	0.876(6)
O(10)	0.140(3)	−0.017(1)	1.404(3)	C(15)	0.388(5)	−0.065(2)	0.737(5)
N(1)	0.332(3)	0.005(1)	0.914(3)	C(16)	0.384(7)	−0.092(3)	1.265(7)
N(2)	0.347(4)	−0.017(2)	1.156(4)				

Table 6 Atomic coordinates with e.s.d.s of cluster **3**

Atom	*x*	*y*	*z*	Atom	*x*	*y*	*z*
Os(1)	0.344 1(1)	0.250 0	0.471 66(9)	C(1)	0.564(4)	0.250 0	0.534(3)
Os(2)	0.027 4(1)	0.250 0	0.316 30(8)	C(2)	0.309(4)	0.250 0	0.612(3)
Os(3)	0.338 1(1)	0.250 0	0.234 66(8)	C(3)	0.333(2)	0.394(1)	0.464(2)
S(1)	0.131 8(4)	0.363 6(3)	0.213 6(4)	C(4)	−0.012(2)	0.151(1)	0.411(2)
O(1)	0.693(3)	0.250 0	0.567(2)	C(5)	−0.178(3)	0.250 0	0.204(2)
O(2)	0.273(3)	0.250 0	0.692(2)	C(6)	0.489(2)	0.146(1)	0.278(2)
O(3)	0.324(2)	0.472(1)	0.457(1)	C(7)	0.326(3)	0.250 0	0.076(3)
O(4)	−0.041(2)	0.094(1)	0.469(1)	C(8)	0.008(2)	0.372(1)	0.058(2)
O(5)	−0.305(2)	0.250 0	0.154(2)	C(9)	−0.227(4)	0.388(2)	−0.091(3)
O(6)	0.575(2)	0.086(1)	0.303(1)	C(10)	−0.386(5)	0.414(3)	−0.090(4)
O(7)	0.346(2)	0.250 0	−0.015(2)	C(11)	−0.155(4)	0.391(2)	−0.152(3)
N(1)	−0.141(2)	0.386(1)	0.042(2)	C(12)	−0.022(3)	0.390(2)	−0.135(2)
N(2)	0.079(2)	0.383(1)	−0.014(2)	C(13)	0.070(4)	0.413(3)	−0.207(3)

Table 7 Selected bond lengths (Å) and angles (°) of cluster **3**

Os(1)–Os(2)	2.899(1)	Os(1)–Os(3)	2.890(1)
Os(2)–S(1)	2.435(4)	Os(3)–S(1)	2.438(4)
S(1)–C(8)	1.85(2)	N(1)–C(8)	1.35(2)
N(2)–C(8)	1.29(2)		
Os(2)–Os(1)–Os(3)	71.82(3)	Os(1)–Os(3)–S(1)	80.70(10)
Os(2)–S(1)–Os(3)	88.3(1)	S(1)–Os(3)–S(1)	81.0(2)

picture in **1** exhibited by two sulfur bridging ligands is rarely observed in metal carbonyl clusters.

An ORTEP drawing of the cluster $[Os_3(CO)_{10}(\mu\text{-SH})(\mu\text{-dmpymt})]$ **2** is depicted in Fig. 4. Final atomic coordinates are listed in Table 4 and selected bond lengths and angles are listed in Table 5. The molecular structure consists of an open triangular array of osmium atoms with two approximate equidistant edges of Os(1)–Os(2) [2.869(2) Å] and the Os(2)–Os(3) [2.870(2) Å]. The remaining Os(1)–Os(3) is a non-bonding distance of 3.320(2) Å. The Os(1)–S(2) [2.49(1) Å] and the Os(3)–S(2) distances [2.51(1) Å] of the bridging thio moiety are significantly longer than the Os(1)–S(1) [2.40(1) Å] and the Os(3)–S(1) [2.43(1) Å] distances of the bridging dmpymt group. The S(1)···S(2) distance [3.21(2) Å] is slightly longer than that in **1** [3.18(1) Å]. In contrast to the cluster **1**, the Os(1)–Os(3) edge is doubly bridged by a dmpymt moiety and a thio ligand, as shown in Fig. 4. However, the salient feature of **2** is that one of the dmpymt moieties has undergone C–S bond cleavage upon co-ordinating to the cluster framework whilst the second dmpymt moiety remains intact on the cluster. We have recently shown that similar C–S bond cleavage has been observed when the dmpymt ligand is added to the osmium cluster under ambient conditions.[15] These results have led us to suspect that bridging co-ordination of the ligand would facilitate the C–S bond cleavage. Adams and Pompeo[30] have proposed that, during the reaction between $[Os_3(CO)_{10}(MeCN)_2]$ and thietane ($\overbrace{SCH_2CH_2CH_2}$), the cluster framework withdraws electrons from the adjacent carbon–sulfur bond to such extent that cleavage of the C–S bond becomes facile. This observation prompted us to investigate the thermal reaction of **1**. Cluster **1** was thermolysed in refluxing *n*-hexane (69 °C) but **1** remained unchanged after 5 h of heating. Furthermore, photochemical activation resulted in the decomposition of **1**. Therefore, **1** may not be a precursor of **2**.

Thermolysis of **1** in refluxing *n*-heptane (98 °C) afforded different products depending on the reaction time. Cluster $[Os_3(CO)_{10}(\mu\text{-dmpymt})_2]$ **3** was the major product (62%) for reaction times of < 1 h. Both ^{1}H NMR and FAB MS indicated that the two dmpymt moieties are still retained in **3**. To elucidate the structure of **3**, a single-crystal X-ray diffraction study was carried out. The molecular structure of **3** is depicted in Fig. 5. Atomic coordinates and selected bonding parameters

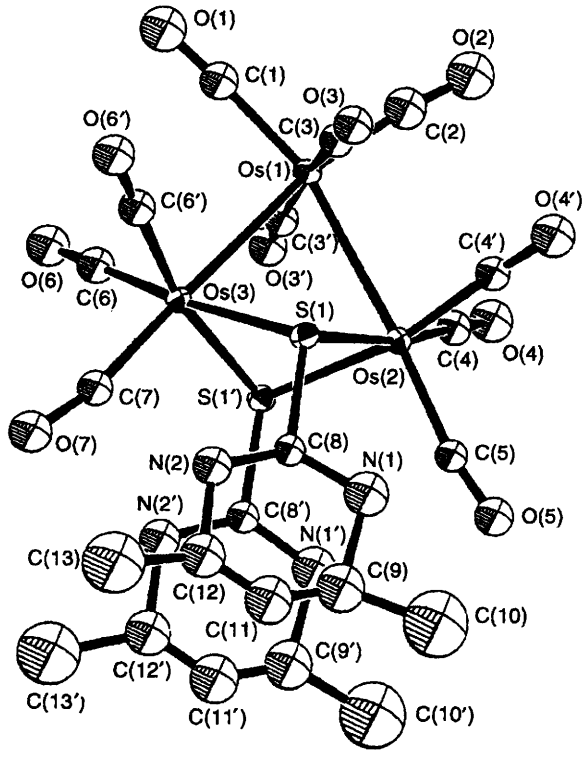

Fig. 5 An ORTEP drawing of $[Os_3(CO)_{10}(\mu\text{-dmpymt})_2]$ **3**

are summarized in Tables 6 and 7 respectively. Cluster **3** possesses an approximate C_{2v} idealized symmetry with the three osmium atoms arranged in an isosceles manner [Os(1)–Os(2) 2.899(1) Å *vs.* Os(1)–Os(3) 2.890(1) Å]. The twelve methyl protons thus are equivalent and give rise to a singlet in the ^{1}H NMR spectrum. The two dmpymt moieties have rearranged to bridge along the same Os–Os edge in the mode **C**. Both dmpymt ligands still behave as three-electron donors. We have recently isolated the ruthenium analogue of **3**, $[Ru_3(CO)_{10}(\mu\text{-dmpymt})_2]$, which also possesses a similar structural geometry to **3**.[15] The average Os–S [2.437(4) Å] and S···S distances [3.166(8) Å] in **3** do not differ significantly from their corresponding values, 2.434(4) and 3.171(6) Å respectively, in $[Ru_3(CO)_{10}(\mu\text{-dmpymt})_2]$.

Cluster **3** underwent decarbonylation and transformed into two new clusters $[Os_3(CO)_9(\mu\text{-dmpymt})(\mu_3\text{-}\eta^2\text{-dmpymt})]$ **4** (42%) and $[Os_3(CO)_8(\mu\text{-}\eta^2\text{-dmpymt})(\mu_3\text{-}\eta^2\text{-dmpymt})]$ **5** (9%) when heated to reflux in *n*-heptane (98 °C) for 2 h. Compound **4** has been characterized by IR, ^{1}H NMR, FAB MS and single-crystal X-ray diffraction analysis and an ORTEP drawing of its molecular structure is shown in Fig. 6. Final atomic

Table 8 Atomic coordinates with e.s.d.s of cluster **4**

Atom	*x*	*y*	*z*	Atom	*x*	*y*	*z*
Os(1)	0.522 31(5)	0.211 68(2)	0.390 66(4)	C(3)	0.435(1)	0.288 8(7)	0.430(1)
Os(2)	0.525 29(5)	0.267 08(3)	0.191 17(4)	C(4)	0.472(1)	0.186 1(7)	0.137(1)
Os(3)	0.770 55(5)	0.214 80(3)	0.222 51(4)	C(5)	0.564(1)	0.298 8(8)	0.060(1)
S(1)	0.646 8(3)	0.127 8(2)	0.303 6(2)	C(6)	0.355(1)	0.292 9(8)	0.205(1)
S(2)	0.723 3(3)	0.270 4(2)	0.386 2(3)	C(7)	0.936(1)	0.182 8(7)	0.263(1)
O(1)	0.547(1)	0.171 7(6)	0.618(1)	C(8)	0.835(1)	0.292 3(8)	0.164(1)
O(2)	0.293(1)	0.127 0(6)	0.351 0(9)	C(9)	0.772(1)	0.171 4(8)	0.100(1)
O(3)	0.376(1)	0.334 9(6)	0.450(1)	C(10)	0.736(1)	0.079 9(6)	0.393 6(9)
O(4)	0.444(1)	0.134 9(6)	0.107 1(9)	C(11)	0.915(1)	0.023 9(8)	0.427(1)
O(5)	0.591(1)	0.312 3(7)	−0.027(1)	C(12)	0.865(1)	0.004 0(8)	0.517(1)
O(6)	0.248(1)	0.306 1(8)	0.208(1)	C(13)	0.744(1)	0.026 1(8)	0.543(1)
O(7)	1.037(1)	0.173 2(6)	0.282(1)	C(14)	1.048(2)	0.005 9(8)	0.391(2)
O(8)	0.864(1)	0.339 4(7)	0.121(1)	C(15)	0.682(2)	0.007(1)	0.642(2)
O(9)	0.768(1)	0.145 3(7)	0.018(1)	C(16)	0.687(1)	0.350 9(7)	0.342(1)
N(1)	0.852 7(9)	0.063 4(6)	0.364 5(9)	C(17)	0.732(1)	0.461 3(8)	0.357(1)
N(2)	0.679(1)	0.063 2(6)	0.476 6(8)	C(18)	0.637(1)	0.472 8(9)	0.286(1)
N(3)	0.754(1)	0.400 0(6)	0.386 1(9)	C(19)	0.577(1)	0.422 2(8)	0.240(1)
N(4)	0.602(1)	0.359 9(5)	0.264 5(9)	C(20)	0.805(2)	0.518 8(8)	0.405(1)
C(1)	0.543(1)	0.180 2(7)	0.527(1)	C(21)	0.469(2)	0.437 9(9)	0.159(1)
C(2)	0.380(1)	0.161 8(7)	0.370(1)				

Table 9 Selected bond lengths (Å) and angles (°) of cluster **4**

Os(1)–Os(2)	2.8323(7)	Os(2)–Os(3)	2.8365(7)
Os(1)–S(1)	2.427(3)	Os(1)–S(2)	2.439(3)
Os(3)–S(1)	2.432(3)	Os(3)–S(2)	2.463(4)
Os(2)–N(4)	2.26(2)	S(2)–C(16)	1.77(1)
S(1)–C(10)	1.79(1)	C(10)–N(1)	1.33(2)
C(16)–N(3)	1.36(2)	C(16)–N(4)	1.36(2)
Os(1)–Os(2)–Os(3)	74.42(2)	Os(1)–S(2)–Os(3)	88.7(1)
Os(1)–S(1)–Os(3)	89.7(1)	Os(2)–Os(3)–S(2)	76.68(8)
Os(2)–Os(1)–S(2)	77.12(8)	Os(2)–Os(1)–S(1)	80.68(8)
Os(2)–Os(3)–S(1)	80.52(7)	S(1)–Os(1)–S(2)	81.5(2)
S(1)–Os(3)–S(2)	76.68(8)		

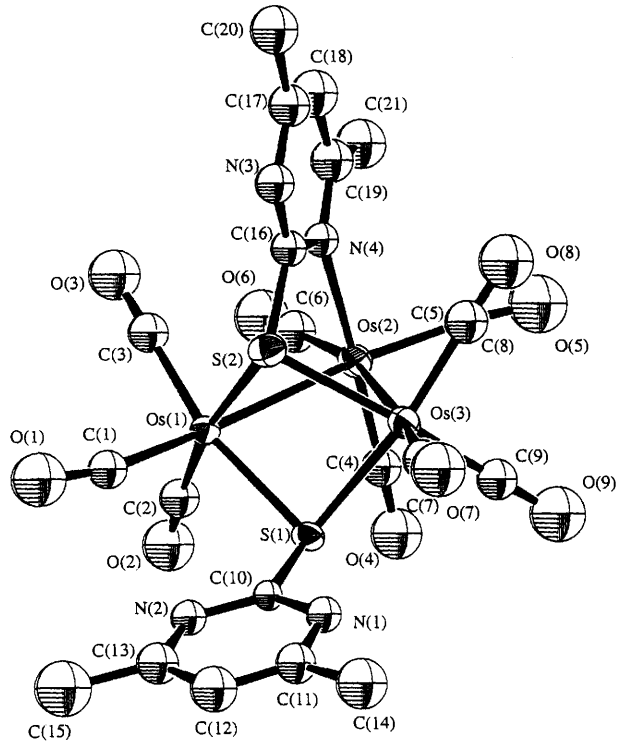

Fig. 6 An ORTEP drawing of $[Os_3(CO)_9(\mu\text{-dmpymt})(\mu_3\text{-}\eta^2\text{-dmpymt})]$ **4**

positional parameters are listed in Table 8 and selected bonding parameters are listed in Table 9. Cluster **4** consists of a triangular array of three osmium metal atoms but has only nine terminal carbonyl ligands, three on each metal atom. One of the bridging dmpymt ligands in **3** has been transformed into a triply bridging ligand through the additional co-ordination of one nitrogen atom. This μ_3-η^2 co-ordination mode **E** of dmpymt has been observed in $[Ru_3(CO)_9(\mu_3\text{-}\eta^2\text{-dmpymt})]$[15] and $[Cu_6(dmpymt)_6]$.[22] Similar bonding modes have also been found in metal clusters containing pyridine-2-thione,[4,13] thioamides[14] and quinoline-2-thione.[13] The Os(2)–Os(3) [2.8365(7) Å] and Os(1)–Os(2) [2.8323(7) Å] distances are slightly shorter than the average Os–Os bond distance in $[Os_3(CO)_{12}]$ [2.877(3) Å].[31] The Os(3)–S(2) distance [2.463(4) Å] is significantly longer than that of Os(1)–S(2) [2.439(3) Å] by almost 0.03 Å which features the asymmetric bridging nature of the S(2) atom. The Os(2)–N(4) distance [2.26(2) Å] is comparable to that found in $[Os_3(CO)_9(\mu\text{-H})\{\mu_3\text{-SC(NPh)(NHPh)}\}]$ [2.25(1) Å][32] while the S···S distance in **4** [3.174(1) Å] is relatively longer than that in **3** [3.166(8) Å].

Curiously, cluster **4** may result from the flipping transformation of one of the bridging dmpymt ligands in **3** into a capping mode over the osmium triangle so that formation of the Os(2)–N(4) bond is feasible. This is accompanied by the elimination of the axial carbonyl of Os(2) so that the octahedral geometry around the Os(2) is essentially preserved, as illustrated in Scheme 1. To our knowledge, **4** is the only example in which two different bonding modes, **C** and **E**, of pymt-type ligands occur within the same cluster framework.

Crystals suitable for X-ray structural analysis of the minor product $[Os_3(CO)_8(\mu\text{-}\eta^2\text{-dmpymt})(\mu_3\text{-}\eta^2\text{-dmpymt})]$ **5** can only be obtained by repeated fractional crystallization. In view of the fact that the structure of **5** differs from that of **4** in the displacement of one carbonyl ligand at Os(3), we believe that **4** may be a precursor of **5**. To verify this, **4** was thermolysed in *n*-octane (125 °C) for 30 min and an almost quantitative conversion to **5** was observed.

Cluster **5** has been characterized by IR, ^{1}H NMR, FAB MS as well as single-crystal X-ray diffraction analysis. There are two crystallographically independent molecules within the asymmetric unit and an ORTEP drawing of molecule 1 of **5** is shown in Fig. 7. Final atomic positional parameters are listed in Table 10 and selected bonding parameters are listed in Table 11. As in **4**, cluster **5** consists of an open triangle of osmium atoms with three linear terminal carbonyl ligands on Os(1) and Os(2)

Table 10 Atomic coordinates with e.s.d.s of cluster **5**

Atom	*x*	*y*	*z*	Atom	*x*	*y*	*z*
Os(1)	−0.016 12(6)	0.017 46(3)	0.182 13(4)	C(4)	0.097(2)	0.132 3(8)	0.237(1)
Os(2)	0.120 00(6)	0.076 36(3)	0.288 62(4)	C(5)	0.222(2)	0.095 7(7)	0.371(1)
Os(3)	0.126 39(6)	−0.016 57(3)	0.341 19(4)	C(6)	0.251(2)	0.061 5(8)	0.246(1)
Os(4)	−0.495 63(7)	0.234 26(3)	0.788 10(4)	C(7)	0.287(2)	−0.017 6(7)	0.373(1)
Os(5)	−0.427 85(6)	0.283 83(3)	0.668 65(4)	C(8)	0.114(2)	0.005 2(7)	0.430(1)
Os(6)	−0.456 86(6)	0.187 39(3)	0.632 60(4)	C(9)	−0.371(2)	0.256 1(8)	0.854(1)
Cl(1)	−0.130 5(9)	0.088 6(4)	−0.025 8(6)	C(10)	−0.559(2)	0.193 9(8)	0.857(1)
Cl(2)	−0.355 2(9)	0.051 7(4)	0.006 0(6)	C(11)	−0.583(2)	0.289 0(8)	0.795(1)
S(1)	−0.090 5(4)	−0.006 5(2)	0.291 8(2)	C(12)	−0.383(2)	0.295 6(8)	0.580(1)
S(2)	0.145 6(4)	−0.043 2(2)	0.218 0(3)	C(13)	−0.268(2)	0.271 4(8)	0.707(1)
S(3)	−0.639 9(4)	0.204 1(2)	0.686 4(3)	C(14)	−0.420(2)	0.344 7(8)	0.712(1)
S(4)	−0.358 8(4)	0.169 4(2)	0.757 7(3)	C(15)	−0.320(2)	0.180 6(8)	0.595(1)
O(1)	−0.178(1)	0.104 2(6)	0.161 5(8)	C(16)	−0.537(2)	0.198 1(8)	0.544(1)
O(2)	−0.181(1)	−0.053 2(6)	0.087 6(8)	C(17)	−0.125(1)	0.046 8(6)	0.333 6(8)
O(3)	0.126(1)	0.050 9(6)	0.067 4(9)	C(18)	−0.250(1)	0.085 6(6)	0.397 8(9)
O(4)	0.081(1)	0.169 3(6)	0.207 0(9)	C(19)	−0.179(2)	0.123 8(7)	0.406(1)
O(5)	0.294(1)	0.109 0(6)	0.418 5(9)	C(20)	−0.078(1)	0.123 5(6)	0.372 6(9)
O(6)	0.338(1)	0.053 0(6)	0.221 8(8)	C(21)	−0.371(2)	0.082 0(8)	0.426(1)
O(7)	0.392(1)	−0.013 7(5)	0.396 6(7)	C(22)	0.001(2)	0.166 5(8)	0.383(1)
O(8)	0.111(1)	0.022 1(5)	0.487 9(7)	C(23)	0.072(1)	−0.094 3(6)	0.245 5(9)
O(9)	−0.284(1)	0.267 9(6)	0.897 7(9)	C(24)	−0.025(2)	−0.164 5(7)	0.230(1)
O(10)	−0.603(2)	0.173 4(7)	0.898(1)	C(25)	−0.041(2)	−0.165 6(7)	0.302(1)
O(13)	−0.640(1)	0.326 2(6)	0.801 0(9)	C(26)	0.003(2)	−0.127 3(7)	0.343(1)
O(14)	−0.349(1)	0.302 9(6)	0.523 0(9)	C(27)	−0.078(2)	−0.206 3(9)	0.182(1)
O(15)	−0.167(1)	0.262 6(6)	0.734 9(9)	C(28)	−0.014(2)	−0.120 7(8)	0.420(1)
O(16)	−0.401(1)	0.381 8(6)	0.741 4(9)	C(29)	−0.697(1)	0.254 5(6)	0.635 4(9)
O(17)	−0.229(1)	0.180 5(6)	0.569 3(8)	C(30)	−0.865(2)	0.287 0(7)	0.564(1)
O(18)	−0.587(1)	0.209 9(6)	0.485 3(9)	C(31)	−0.796(2)	0.326 3(7)	0.554(1)
N(1)	−0.223(1)	0.046 2(5)	0.361 8(7)	C(32)	−0.676(2)	0.328 5(7)	0.584(1)
N(2)	−0.045(1)	0.085 0(5)	0.336 0(7)	C(33)	−0.995(2)	0.281 9(8)	0.537(1)
N(3)	0.031(1)	−0.129 7(6)	0.201 2(8)	C(34)	−0.606(2)	0.373 2(8)	0.570(1)
N(4)	0.065(1)	−0.091 9(5)	0.315 0(7)	C(35)	−0.449(1)	0.117 1(7)	0.744 3(9)
N(5)	−0.814(1)	0.250 1(5)	0.607 8(8)	C(36)	−0.571(2)	0.077 8(8)	0.650(1)
N(6)	−0.622(1)	0.291 9(5)	0.624 9(7)	C(37)	−0.591(2)	0.044 0(7)	0.700(1)
N(7)	−0.465(1)	0.086 7(5)	0.793 5(8)	C(38)	−0.537(2)	0.048 0(7)	0.771(1)
N(8)	−0.496(1)	0.115 7(5)	0.673 1(7)	C(39)	−0.634(2)	0.075 3(8)	0.575(1)
C(1)	−0.114(2)	0.070 0(7)	0.170(1)	C(40)	−0.558(2)	0.014 8(9)	0.828(1)
C(2)	−0.117(2)	−0.028 3(8)	0.127(1)	C(41)	−0.283(3)	0.089(1)	−0.050(2)
C(3)	0.069(2)	0.037 4(8)	0.110(1)				

Table 11 Selected bond lengths (Å) and angles (°) of cluster **5**

Molecule 1		Molecule 2	
Os(1)–Os(2)	2.833(2)	Os(4)–Os(5)	2.845(1)
Os(2)–Os(3)	2.761(2)	Os(5)–Os(6)	2.769(2)
Os(1)–S(1)	2.443(5)	Os(4)–S(3)	2.444(4)
Os(1)–S(2)	2.487(5)	Os(4)–S(4)	2.494(6)
Os(3)–S(1)	2.476(4)	Os(6)–S(3)	2.479(5)
Os(3)–S(2)	2.478(5)	Os(6)–S(4)	2.481(5)
Os(2)–N(2)	2.20(1)	Os(5)–N(6)	2.21(1)
Os(3)–N(4)	2.24(1)	Os(6)–N(8)	2.20(1)
S(1)–C(5)	1.76(2)	S(3)–C(29)	1.76(2)
S(2)–C(23)	1.76(2)	S(4)–C(35)	1.76(2)
Os(1)–Os(2)–Os(3)	72.15(3)	Os(4)–Os(5)–Os(6)	71.92(3)
Os(1)–S(1)–Os(3)	84.1(1)	Os(4)–S(3)–Os(6)	84.1(1)
Os(1)–S(2)–Os(3)	83.1(2)	Os(4)–S(4)–Os(6)	83.1(1)
S(1)–Os(1)–S(2)	85.6(2)	S(3)–Os(4)–S(4)	85.8(2)
S(1)–Os(3)–S(2)	85.1(1)	S(3)–Os(6)–S(4)	85.3(2)

and two on Os(3). The Os(1)–Os(2) [2.833(2) Å] and the Os(2)–Os(3) distances [2.761(2) Å] are slightly shorter than the average metal–metal distance of 2.877(3) Å found in $[Os_3(CO)_{12}]$.[31] The Os(1)–S(1) [2.443(5) Å] and Os(3)–S(1) [2.487(5) Å] distances differ by more than 0.03 Å which is greater than that found in **4**; thus asymmetric bridging of S(1) to Os(1) and Os(3) is more pronounced. The Os(2)–N(2) distance [2.20(1) Å], the Os(1)–S(2)–Os(3) angle [83.1(2)°] and the Os(1)–S(1)–Os(3) angle [84.1(1)°] are significantly diminished

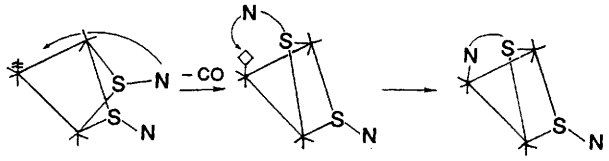

Scheme 1 Proposed mechanism for the formation of cluster **4** from **3**

as compared with their corresponding values in **4** [2.26(2) Å, 89.7(1)° and 88.7(1)°] respectively. Of the two dmpymt ligands in the cluster framework of **5**, one exhibits the conventional μ_3-η^2 mode **E** whilst the other co-ordinates in a five electron-donating μ-η^2 fashion, see Fig. 8. It is worth noting that this new doubly-bridging donating mode is seldom observed for pyrimidine-2-thione type ligands in trinuclear or other higher nuclearity clusters but a comparable example can be found for pyridine-2-thione type ligands.[33] The resulting geometry around Os(3) can be described as distorted octahedral with an S(2)–Os(3)–N(4) angle of 65.4(4)°. The S(1) • • • S(2) distance is 3.34(1) Å and is longer than those in cluster **1** [3.17(1) Å], **2** [3.21(2) Å], **3** [3.166(8) Å] and **4** [3.17(1) Å].

As already mentioned above, **4** undergoes CO displacement to give **5**. We believed that the backward conversion from **5** to **4** may also be feasible; when a stream of CO was bubbled through a CH_2Cl_2 solution of **5** for 3 h, cluster **4** was obtained as the major product (62%). Conversion of **4** into **5** is thus reversible. However, attempts to convert **4** to **3** occurred only in refluxing *n*-hexane (69 °C) and with a much lower yield (27%).

Table 12 Atomic coordinates with e.s.d.s of cluster **6**

Atom	*x*	*y*	*z*	Atom	*x*	*y*	*z*
Os(1)	0.805 9(1)	0.037 88(7)	0.825 22(10)	C(1)	0.955(4)	0.043(2)	0.869(3)
Os(2)	0.789 3(1)	0.128 77(7)	0.925 8(1)	C(2)	0.827(3)	−0.001(2)	0.737(3)
Os(3)	0.827 0(2)	0.142 80(7)	0.759 3(1)	C(3)	0.797(4)	−0.024(2)	0.890(3)
Os(4)	0.742(1)	0.010 66(7)	0.300 1(1)	C(4)	0.658(3)	0.044(1)	0.786(2)
Os(5)	0.826 4(1)	0.087 43(7)	0.420 70(9)	C(5)	0.883(5)	0.090(3)	1.002(4)
Os(6)	0.674 2(1)	0.121 40(7)	0.261 01(9)	C(6)	0.685(3)	0.086(2)	0.949(2)
S(1)	0.686 5(8)	0.163 3(4)	0.812 6(6)	C(7)	0.775(4)	0.194(2)	0.990(3)
S(2)	0.924 7(9)	0.172 6(6)	0.881(1)	C(8)	0.746(4)	0.126(2)	0.666(3)
S(3)	0.850 3(8)	0.139 5(4)	0.315 5(6)	C(9)	0.943(3)	0.117(2)	0.728(2)
S(4)	0.660 9(9)	0.131 5(4)	0.390 5(6)	C(10)	0.862(3)	0.023(1)	0.261(2)
O(1)	1.033(3)	0.050(2)	0.896(2)	C(11)	0.664(3)	−0.022(2)	0.210(3)
O(2)	0.835(3)	−0.020(1)	0.687(2)	C(12)	0.801(3)	−0.054(2)	0.352(2)
O(3)	0.782(3)	−0.060(2)	0.924(2)	C(13)	0.627(3)	0.006(2)	0.342(2)
O(4)	0.576(3)	0.044(1)	0.763(2)	C(14)	0.786(3)	0.036(2)	0.487(3)
O(5)	0.939(4)	0.069(2)	1.044(3)	C(15)	0.883(3)	0.139(2)	0.498(2)
O(6)	0.613(3)	0.063(1)	0.954(2)	C(16)	0.949(2)	0.046(1)	0.428(2)
O(7)	0.779(3)	0.223(2)	1.038(2)	C(17)	0.697(3)	0.118(2)	0.168(3)
O(8)	0.695(3)	0.115(2)	0.613(3)	C(18)	0.538(3)	0.096(2)	0.221(2)
O(9)	1.007(3)	0.099(1)	0.706(2)	C(19)	0.660(3)	0.240(2)	0.818(3)
O(10)	0.920(2)	0.031(1)	0.232(2)	C(20)	0.646(4)	0.321(2)	0.885(3)
O(11)	0.620(2)	−0.035(1)	0.153(2)	C(21)	0.606(4)	0.340(2)	0.823(3)
O(12)	0.839(2)	−0.093(1)	0.383(2)	C(22)	0.591(4)	0.315(2)	0.755(3)
O(13)	0.568(2)	0.005(1)	0.371(2)	C(23)	0.662(4)	0.343(2)	0.959(3)
O(14)	0.757(2)	0.006(1)	0.523(2)	C(24)	0.542(5)	0.339(3)	0.686(4)
O(15)	0.913(2)	0.167(1)	0.547(2)	C(25)	0.884(3)	0.244(2)	0.827(3)
O(16)	1.018(2)	0.023(1)	0.426(2)	C(26)	0.876(4)	0.326(2)	0.820(3)
O(17)	0.718(2)	0.117(1)	0.112(2)	C(27)	0.834(4)	0.333(3)	0.752(4)
O(18)	0.467(3)	0.079(2)	0.189(2)	C(28)	0.822(4)	0.282(2)	0.708(3)
N(1)	0.673(2)	0.261(1)	0.884(2)	C(29)	0.887(7)	0.386(4)	0.870(5)
N(2)	0.619(3)	0.259(2)	0.750(2)	C(30)	0.776(5)	0.263(3)	0.642(4)
N(3)	0.912(4)	0.288(2)	0.891(3)	C(31)	0.883(3)	0.212(2)	0.334(2)
N(4)	0.847(3)	0.234(2)	0.763(2)	C(32)	0.903(3)	0.297(2)	0.286(2)
N(5)	0.874(2)	0.243(1)	0.273(2)	C(33)	0.946(3)	0.318(2)	0.353(2)
N(6)	0.916(2)	0.228(1)	0.402(2)	C(34)	0.946(3)	0.283(2)	0.410(2)
N(7)	0.681(2)	0.247(1)	0.416(2)	C(35)	0.897(3)	0.331(2)	0.214(3)
N(8)	0.650(2)	0.208(1)	0.293(2)	C(36)	0.987(4)	0.302(2)	0.490(3)

Table 13 Selected bond lengths (Å) and angles (°) of cluster **6**

Molecule 1		Molecule 2	
Os(1)–Os(2)	2.902(2)	Os(4)–Os(5)	2.906(2)
Os(1)–Os(3)	2.822(2)	Os(4)–Os(6)	2.827(2)
Os(2)–S(1)	2.39(1)	Os(5)–S(3)	2.406(10)
Os(2)–S(2)	2.47(1)	Os(5)–S(4)	2.47(1)
Os(3)–S(1)	2.45(1)	Os(6)–S(3)	2.45(1)
Os(3)–S(2)	2.45(2)	Os(6)–S(4)	2.48(1)
Os(3)–N(4)	2.19(4)	Os(6)–N(8)	2.19(3)
S(1)–C(19)	1.86(4)	S(3)–C(31)	1.79(4)
S(2)–C(25)	1.99(5)	S(4)–C(37)	1.78(4)
C(25)–N(4)	1.21(5)	C(37)–N(8)	1.38(4)
Os(2)–Os(1)–Os(3)	70.07(6)	Os(5)–Os(4)–Os(6)	70.11(3)
Os(2)–S(1)–Os(3)	85.6(3)	Os(5)–S(3)–Os(6)	85.8(3)
Os(2)–S(2)–Os(3)	83.8(4)	Os(5)–S(4)–Os(6)	84.0(3)
S(1)–Os(2)–S(2)	84.4(5)	S(3)–Os(5)–S(4)	84.3(3)
S(1)–Os(3)–S(2)	83.4(4)	S(3)–Os(6)–S(4)	83.2(4)
S(2)–Os(3)–N(4)	69(1)	S(4)–Os(6)–N(8)	65 9(8)
Os(3)–S(2)–C(25)	75(1)	Os(6)–S(4)–C(37)	81(1)

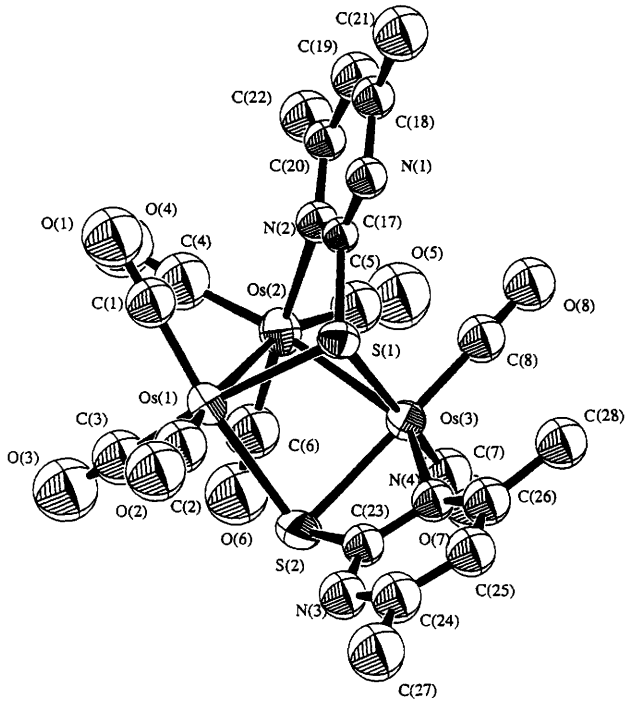

Fig. 7 An ORTEP drawing of $[Os_3(CO)_8(\mu\text{-}\eta^2\text{-dmpymt})(\mu_3\text{-}\eta^2\text{-dmpymt})]$ **5**

On the other hand, we found that reaction of a stoichiometric amount of **1** with Me_3NO at −78 °C afforded two products; TLC purification and spectroscopic measurements confirmed that some starting material **1** was still present but that a mixture of clusters **3** and **4** (IR and ^1H NMR) were also obtained. Attempts to purify the remaining uncharacterized orange product were unsuccessful. When an excess of Me_3NO was employed, the yield of **3** and **4** increased at the expense of **1**.

Cluster **4** isomerized quantitatively into another cluster $[Os_3(CO)_9(\mu\text{-dmpymt})(\mu\text{-}\eta^2\text{-dmpymt})]$ **6** (87%) over a period of 10 days at ambient conditions. This isomerization was

Table 14 Crystal data for clusters **1–6**

Cluster	**1**	**2**	**3**	**4**	**5**	**6**
Empirical formula	$C_{22}H_{14}N_4O_{10}Os_3S_2$	$C_{16}H_8N_2O_{10}Os_3S_2$	$C_{22}H_{14}N_4O_{10}Os_3S_2$	$C_{21}H_{14}N_4O_9Os_3S_2$	$2C_{20}H_{14}N_4O_8Os_3S_2{\cdot}CH_2Cl_2$	$2C_{21}H_{14}N_4O_9Os_3S_2$
M	1129.11	1022.97	1129.09	1101.10	2231.10	2202.17
Colour	Deep yellow	Yellow	Pale yellow	Orange	Deep orange	Pale orange
Crystal size (mm)	0.15 × 0.15 × 0.20	0.12 × 0.26 × 0.34	0.24 × 0.26 × 0.34	0.10 × 0.15 × 0.15	0.07 × 0.10 × 0.15	0.10 × 0.15 × 0.20
Crystal system	Monoclinic	Monoclinic	Monoclinic	Orthorhombic	Monoclinic	Monoclinic
Space group	$P2_1/n$	$P2_1/n$	$P2_1/m$	$P2_12_12_1$	$P2_1/c$	$P2_1/n$
a/Å	9.371(2)	10.223(5)	9.357(1)	10.608(6)	11.227(2)	13.918(4)
b/Å	19.887(4)	24.861(3)	13.932(1)	20.147(4)	27.772(3)	23.718(8)
c/Å	15.815(5)	9.298(3)	12.277(1)	13.048(2)	18.826(3)	18.631(7)
β/°	92.74(2)	90.05(3)	110.81(1)	90.00(1)	99.42(1)	103.93(3)
U/Å^3	2943.9(1)	2363(1)	1495.9(2)	2788.6(1)	5790.7(1)	5969(3)
Z	4	4	2	4	4	4
D_c/g cm^{-3}	2.547	2.875	2.506	2.623	2.559	2.45
Absorption coefficient (μ/cm^{-1})	31.297	163.10	128.98	138.55	134.33	129.23
F(000)	2056	1832	1028	2000	4056	4000
Diffractometer	Nonius CAD4	Rigaku AFC7R	Rigaku AFC7R	Nonius CAD4	Nonius CAD4	Rigaku AFC7R
T/K	298	293	293	298	298	298
2θ range/°	2–46	2–45	2–50	2–45	2–45	2–40
Scan speed (°/min^{-1})	1.83–8.24	16	16	1.37–8.24	0.97–8.24	16
Scan range (ω/°)	(0.95 + 0.34 tan θ)	(0.94 + 0.35 tan θ)	(1.42 + 0.35 tan θ)	(1.37 + 0.34 tan θ)	(0.50 + 0.34 tan θ)	(1.31 + 0.35 tan θ)
Reflections collected	4529	3372	2935	4004	6888	5963
Independent reflections	4236	3170	2760	2110	6531	5622
Observed reflections [$I \geqslant 3\sigma(I)$]	3112	2633	1978	1932	4028	3965
Transmission	0.611–0.884	0.610–1.000	0.740–1.000	0.595–0.872	0.731–0.908	0.4939–1.000
p In weighting scheme[b]	0.040	0.000	0.000	0.065	0.060	0.010
R, R_w	0.028, 0.037	0.080, 0.097	0.045, 0.046	0.031, 0.042	0.035, 0.045	0.071, 0.079
Goodness of fit	1.160	2.371	3.110	1.028	1.070	5.18
Largest Δ/σ	0.01	0.05	0.06	0.05	0.05	0.03
No. of parameters	370	158	108	182	359	363
Residual extrema in final difference map (e Å^{-3})	1.10, −1.14	2.73, −3.49	1.79, −1.19	0.81, −1.42	1.18, −1.03	2.82, −3.10

[a] Data in common: Radiation Mo-Kα (λ = 0.710 73 Å), scan type ω–2θ, background measurement extended 25% on each side. [b] Weighting scheme: $4F_o^2/[\sigma^2(F_o^2) + (pF_o^2)]$.

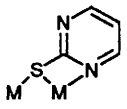

Fig. 8 The μ-η^2 five electron-donating bonding mode of the Hpymt-type ligand

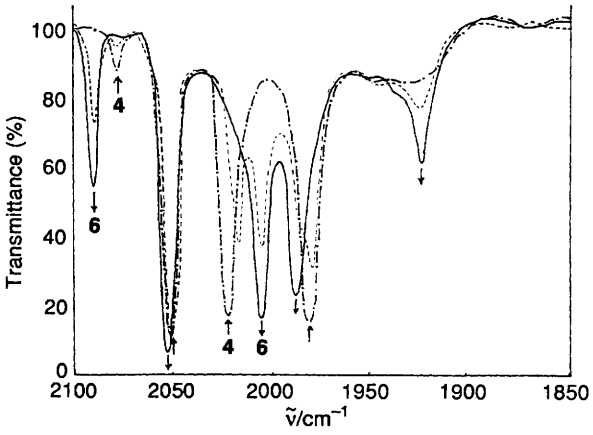

Fig. 9 IR monitoring [ν(CO)(cm^{-1})] of the isomerization of cluster **4** into **6** in CH_2Cl_2

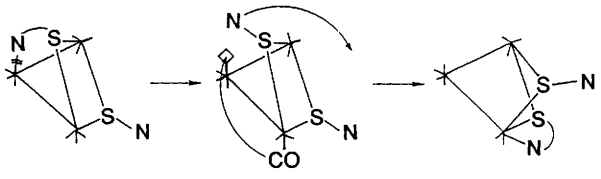

Scheme 2 Proposed mechanism for the formation of cluster **6** from **4**

monitored by IR as shown in Fig. 9; attempts to accelerate the isomerization in refluxing *n*-hexane failed. It is probable that a higher reaction temperature, alternative reaction pathways are more favourable than isomerization. Within the asymmetric unit there are two independent molecules and an ORTEP drawing of molecule 1 of **6** is shown in Fig. 10. Atomic coordinates and bonding parameters are shown in Tables 12 and 13 respectively. The basic structure of **6** consists of an open triangular array of osmium atoms. The Os(1)–Os(2) [2.902(2) Å] and Os(1)–Os(3) [2.822(2) Å] distances are not unusual. The non-bonding Os(2)···Os(3) edge is 3.287(3) Å. Cluster **6** apparently originates from the scission of the Os(2)–N(4) bond in **4** creating a vacant co-ordination site. Flipping of the whole dmpymt moiety from its original face capping μ_3-η^2 bonding E to an *endo* position with respect to the trinuclear plane then proceeds. This must be accompanied by carbonyl migration from Os(3) to the vacant site at Os(2) so that formation of the Os(3)–N(4) bond is feasible. This situation is depicted in Scheme 2. Consequently, the non-bonding Os(2)···Os(3) edge is supported partly by the μ-η^2 bonding mode of the dmpymt ligand as in the case of cluster **5**. A different but related example was found in $[Os_3(CO)_9(\mu\text{-}SCH_2CMe_2CH_2)(\mu\text{-}Cl)]^-$.[34] The S(1)···S(2) distance [3.26(2) Å] is slightly larger than that in **3** [3.166(8) Å]. On the other hand, the Os(3)–N(4) distance [2.19(4) Å] is shorter than that in **5** [2.24(1) Å].

The relationships between clusters **1**–**6** in this work are summarized in Scheme 3 and the spectroscopic data for them are summarized in Table 1. A summary of the crystallographic data for clusters **1**–**6** is also shown in Table 14. All of them

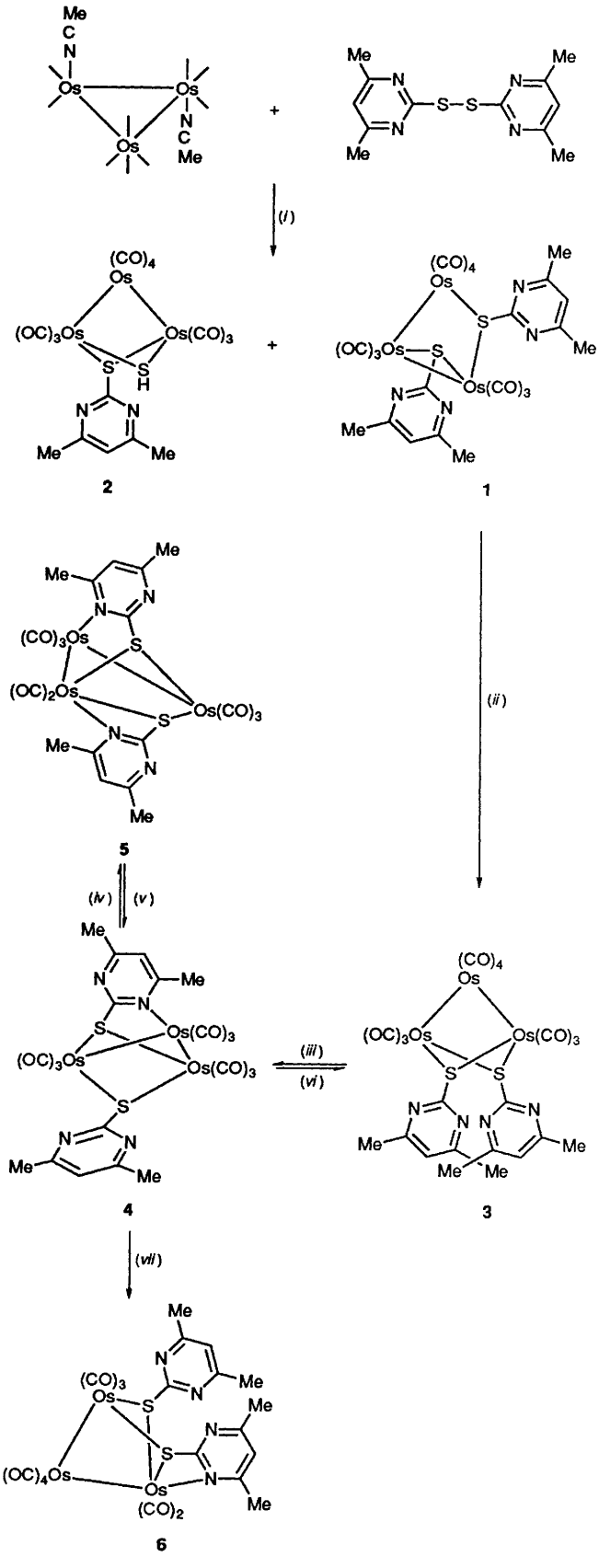

Scheme 3 The relationships between clusters **1**–**6** (*i*) CH_2Cl_2, 25 °C, 1 h; (*ii*) *n*-heptane, 98 °C, 1 h or Me_3NO, CH_2Cl_2, −78 °C; (*iii*) *n*-heptane, 98 °C, 2 h; (*iv*) *n*-octane, 125 °C, 0.5 h; (*v*) CH_2Cl_2, 25 °C, CO, 3 h; (*vi*) *n*-hexane, 71 °C, CO, 3 h; (*vii*) CH_2Cl_2–*n*-heptane, 25 °C, 10 d

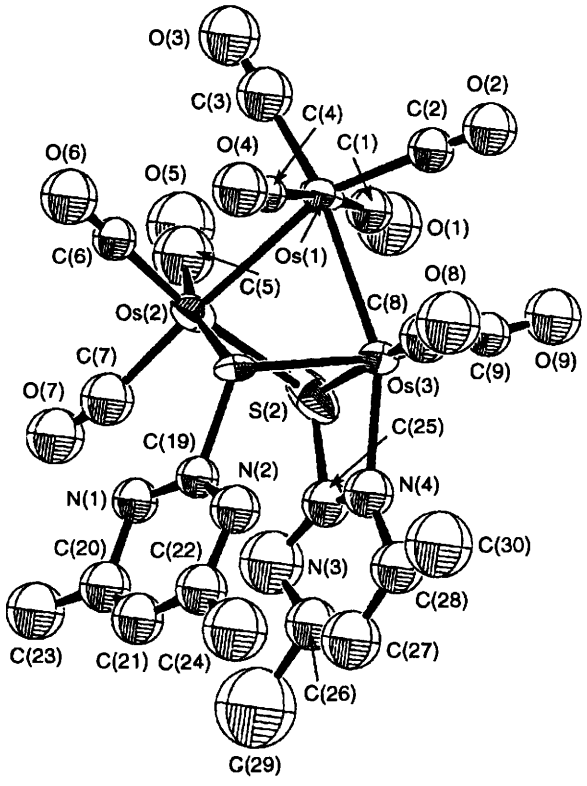

Fig. 10 An ORTEP drawing of $[Os_3(CO)_9(\mu\text{-dmpymt})(\mu\text{-}\eta^2\text{-dmpymt})]$ **6**

Table 15 Non-bonding distances (Å) of S···S and Os···Os in clusters **1**–**6**

Cluster	S···S	Os···Os
1	3.177(3)	3.891(1)
2	3.21(2)	3.320(2)
3	3.166(8)	3.396(1)
4	3.174(5)	3.4281(7)
5	3.347(7), 3.361(6)	3.294(1), 3.297(1)
6	3.26(2), 3.27(1)	3.287(3), 3.310(2)

are trinuclear in which the two dmpymt ligands co-ordinate in different modes. In line with the effective atomic number rule, clusters **1**–**6** all possess a non-bonding metal–metal edge with distances ranging from 3.287(3) Å in **6** to 3.891(1) Å in **1** (Table 15). The bonded osmium–osmium distances fall in the range 2.761(2) Å in **5** to 2.9384(6) Å in **1**; S···S distances adopted by the clusters are also listed in Table 15, and range from 3.166(8) Å in **3** to 3.347(1) Å in **5**; the range is relatively large.

To summarize, cluster **1** underwent isomerization to **3** and subsequently to **4**, **5** and **6** in refluxing *n*-heptane and *n*-octane. Neither the commonly observed stereoisomers of **3**[28] nor the μ^3-bridging SR isomers obtained at higher reaction temperatures could be isolated.[28] Instead, the dmpymt ligands rearranged within the metal framework in different manners as described.

Acknowledgements

W.-T. W. thanks the Hong Kong Research Grants Council and the University of Hong Kong for financial support. Y.-K. A. acknowledges the receipt of a postgraduate studentship, administered by the University of Hong Kong.

References

1 B. F. G. Johnson, J. Lewis and D. A. Pippard, *J. Chem. Soc., Dalton Trans.*, 1981, 407.
2 C. C. Yin and A. J. Deeming, *J. Chem. Soc., Dalton Trans.*, 1975, 2091.
3 R. Zoet, G. van Koten, K. Vrieze, J. Jansen, K. Goubitz and C. H. Stam, *Organometallics*, 1988, **7**, 1565.
4 K. Burgess, B. F. G. Johnson and J. Lewis, *J. Organomet. Chem.*, 1982, **233**, C55.
5 A. J. Arce, Y. D. Sanctis and A. J. Deeming, *J. Organomet. Chem.*, 1986, **311**, 371.
6 A. J. Arce, A. J. Deeming, Y. D. Sanctis, R. Machado, J. Manzur and C. Rivas, *J. Chem. Soc., Chem. Commun.*, 1990, 1568.
7 R. D. Adams, M. P. Pompeo, W. Wu and J. H. Yamamato, *J. Am. Chem. Soc.*, 1993, **115**, 8207.
8 R. D. Adams, J. A. Belinski and J. H. Yamamato, *Organometallics*, 1992, **11**, 3422 and refs. therein.
9 M. W. Day, K. I. Hardcastle, A. J. Deeming, A. J. Arce and Y. D. Sanctis, *Organometallics*, 1990, **9**, 6.
10 R. D. Adams and G. Chen, *Organometallics*, 1992, **11**, 3510.
11 R. D. Adams and G. Chen, *Organometallics*, 1993, **12**, 2070.
12 A. J. Arce, A. J. Deeming, Y. D. Sanctis and J. Manzur, *J. Chem. Soc., Chem. Commun.*, 1993, 325.
13 A. J. Deeming, K. I. Hardcastle and M. Karim, *Inorg. Chem.*, 1992, **31**, 4792.
14 A. M. Brodie, H. D. Holden, J. Lewis and M. J. Taylor, *J. Chem. Soc., Dalton Trans.*, 1986, 633.
15 Y. K. Au, K. K. Cheung and W. T. Wong, *Inorg. Chim. Acta.*, 1995, **228**, 267.
16 A. J. Deeming and R. Vaish, *J. Organomet. Chem.*, 1993, **460**, C8.
17 B. F. G. Johnson, T. M. Layer, J. Lewis, A. Martin and P. R. Raithby, *J. Organomet. Chem.*, 1992, **429**, C41.
18 T. M. Layer, J. Lewis, A. Martin, P. R. Raithby and W. T. Wong, *J. Chem. Soc., Dalton Trans.*, 1992, 3411.
19 E. S. Raper, *Coord. Chem. Rev.*, 1985, **61**, 115.
20 D. M. L. Goodgame, A. M. Z. Slawin, D. J. Williams and P. W. Zard, *Inorg. Chim. Acta*, 1988, **148**, 5; C. Lecomte, St. Sksulika, P. Aslanidis, P. Karagiannidis and St. Papastefanou, *Polyhedron*, 1989, **8**, 1103.
21 J. Abbot, D. M. L. Goodgame and I. Jeeves, *J. Chem. Soc., Dalton Trans.*, 1978, 880; F. A. Cotton and W. H. Isley, *Inorg. Chim. Acta*, 1982, **59**, 213; *Inorg. Chem.*, 1981, **20**, 614.
22 R. Castro, M. L. Duran, J. A. Garcia-Vazquez, J. Romero, A. Sousa, E. E. Castellano and J. Zukerman-Schpector, *J. Chem. Soc., Dalton Trans.*, 1992, 2559.
23 J. N. Nicholls and M. D. Vargas, *Inorg. Synth.*, 1989, **28**, 232.
24 D. T. Hurst, S. G. Jonas, J. Outram and R. A. Patterson, *J. Chem. Soc., Perkin Trans.*, 1977, 1688.
25 A. C. T. North, D. C. Phillips and F. S. Mathews, *Acta Crystallogr., Sect. A*, 1968, **24**, 351.
26 SDP Structure Determination Package, Enraf-Nonius, Delft, 1985.
27 TEXSAN, Crystal Structure Analysis Package, Molecular Structure Corporation, 1985 and 1992.
28 P. V. Broadhurst, B. F. G. Johnson and J. Lewis, *J. Chem. Soc., Dalton Trans.*, 1982, 1881.
29 A. P. Humphries and H. D. Kaesz, *Prog. Inorg. Chem.*, 1979, **2**, 145.
30 R. D. Adams and M. P. Pompeo, *J. Am. Chem. Soc.*, 1991, **113**, 1619.
31 M. R. Churchill and B. G. DeBoer, *Inorg. Chem.*, 1977, **16**, 878.
32 E. W. Ainscough, A. M. Brodie, S. L. Ingham, T. G. Kotch, A. J. Lees, J. Lewis and J. M. Waters, *J. Chem. Soc., Dalton Trans.*, 1994, 1.
33 A. J. Deeming, M. Karim, P. A. Bates and M. B. Hursthouse, *Polyhedron*, 1988, 1401.
34 R. D. Adams, J. A. Belinski and M. P. Pompeo, *Organometallics*, 1991, **10**, 2539.

Received 19*th October* 1994; *Paper* 4/06401A